Further investigation of the photodissociation dynamics of dichlorocarbene near 248 nm

ARTICLE *in* THE JOURNAL OF CHEMICAL PHYSICS · MAY 2008

Impact Factor: 2.95 · DOI: 10.1063/1.2908236 · Source: PubMed

Further investigation of the photodissociation dynamics of dichlorocarbene near 248 nm

Seung Keun Shin and Paul J. Dagdigian[a)]
Department of Chemistry, The Johns Hopkins University, Baltimore, Maryland 21218-2685, USA

(Received 24 December 2007; accepted 20 March 2008; published online 21 April 2008)

A further investigation of the 248 nm photodissociation of CCl_2, which expands upon our original study of this process [S. K. Shin and P. J. Dagdigian, Phys. Chem. Chem. Phys. **8**, 3446 (2006)], is presented. The CCl_2 parent molecule and the CCl photofragment were detected by laser fluorescence excitation in a molecular beam experiment. From the dependence of the CCl_2 signals on the photolysis laser fluence, attenuation cross sections of the 0_0, 1_1, and 2_1 vibrational levels were determined; the cross sections for the excited vibrational levels were found to be significantly smaller than those for the ground vibrational level. The previously observed fragment CCl bimodal rotational state distribution was found to arise from the photolysis of more than one parent molecule. At low $CHCl_3$ mole fractions in the gas supplied to the pyrolysis beam source, it was concluded that CCl_2 is the photolysis precursor for both low-J and high-J CCl fragments. On the basis of the dependence of the CCl signals on the photolysis laser fluence, ground and vibrationally excited CCl_2, respectively, were assigned as the precursors to these two classes of fragments. The photofragment excitation spectra for low-J and high-J CCl fragments from the photolysis of CCl_2 were recorded in the wavelength range around 248 nm; both were found to be structureless. The 248 nm photodissociation dynamics of CCl_2 is discussed in light of our experimental observations and quantum chemical calculations of the CCl_2 excited electronic states. © *2008 American Institute of Physics*. [DOI: 10.1063/1.2908236]

I. INTRODUCTION

Carbenes are an important class of reactive intermediates.[1] While the parent molecule, CH_2, has a triplet ground electronic state, the halocarbenes have singlet ground states. Numerous spectroscopic studies have provided considerable detailed experimental information on the ground $\tilde{X}$ and first excited singlet $\tilde{A}$ states of these species in the gas phase, as exemplified by a number of recent papers.[2–10] By contrast, information on the higher electronic states of the halocarbenes is much more sparse, but some information on their spectroscopy and photochemistry has been gained in recent years. Kable and co-workers have shown that the higher vibrational levels of CFCl and CFBr in the $\tilde{A}$ state dissociate by a curve crossing to yield CF fragments.[11–13] The internal state distribution of CF fragments from the photodissociation of various CFBr($\tilde{A}$) vibronic levels was determined.[13] Recently, Tao *et al.*[10] have observed the quasilinear, predissociative $\tilde{B}$ state of CHF by fluorescence depletion spectroscopy.

Our group has investigated the UV photodissociation dynamics of several halocarbenes.[14–17] Laser fluorescence excitation spectroscopy was employed to characterize the internal state distribution of the CCl and CF fragments from the photolysis of CCl_2 and CFCl, respectively, which were prepared in a pyrolysis molecular beam source. A unique aspect of these experiments is that attenuation cross sections of the parent molecules were determined by monitoring their concentrations by laser fluorescence detection as a function of the fluence of the photolysis laser. These cross sections can be equated with absorption cross sections if the probability of excited-state dissociation is unity. In recent work,[17] the 193 nm photodissociation of CHCl to form CH was investigated; this fragment represents a higher-energy dissociation channel, the lowest involving formation of CCl.

Very different CCl fragment rotational state distributions were observed for the photolysis of CCl_2 at 193 and 248 nm. A modest degree of rotational excitation in CCl($X, v=0$) was observed at the former wavelength.[14] Consideration of the excited electronic states of CCl_2 suggested that a Rydberg state was initially excited and couples, either directly or indirectly, to a repulsive state emanating from the CCl($X\,^2\Pi$) +Cl ground asymptote. By contrast, photolysis at 248 nm was found to yield a bimodal rotational state distribution, peaking at $N \approx 10$ and 85, in the CCl_2 fragments.[15] It was not possible to determine the full rovibrational state distribution of the CCl fragments because the spectroscopy of CCl is not conducive to the laser fluorescence detection of CCl($X, v>0$) molecules.

A very low degree of rotational excitation, with essentially equal A' and A'' Λ-doublet populations and no vibrational excitation, was found for the CF fragment from the 193 nm photolysis of CFCl.[16] As in the case of the 193 nm excitation of CCl_2, the initially excited CFCl electronic state should be a Rydberg state. The low CF rotational excitation, as well as the lack of a Λ-doublet propensity, is consistent with dissociation of a linear intermediate state; a similar con-

a)Author to whom correspondence should be addressed. Electronic mail: pjdagdigian@jhu.edu.

sideration also applies to the CCl fragments from the 193 nm photolysis of CCl_2. We note that the Rydberg states of both CFCl and CCl_2 are expected to be bent based on the geometries of the corresponding cations.[18]

The present study was initiated to explore the previously reported[15] bimodal rotational state distribution of the CCl fragment in the 248 nm photodissociation of CCl_2. Among the questions to be answered was whether the high- and low-*J* fragments involved the initial excitation of two separate electronic states, or alternatively, whether the two classes of fragments were formed by nonadiabatic coupling of a single initially excited state to a second CCl_2 electronic state. To this end, photofragment excitation spectra have been recorded for wavelengths around 248 nm. During the course of this study, we found that there were, in fact, two photolytic sources of the observed low-*J* CCl fragments, involving separate parent molecules with very different 248 nm absorption cross sections. Here we present the relevant data and identify the photolytic precursors. The photofragment excitation spectra show no vibrational structure, suggesting that the excited CCl_2 electronic state accessed by excitation near 248 nm is purely repulsive. We also report 248 nm attenuation cross sections for several vibrational levels of CCl_2 and find significantly differing values.

II. EXPERIMENT

A brief description of the experimental arrangement is provided here since the apparatus has been previously described in detail.[14–16] Dichlorocarbene was generated in a supersonic beam by flash pyrolysis of a dilute mixture of chloroform in argon (total pressure of 1 atm) by passage through a resistively heated 1.5 cm long section of SiC tube (1 mm inner diameter, 2 mm outer diameter) attached to a pulsed solenoid valve (General Valve). The temperature of the SiC tube was estimated from readings of a thermocouple inserted into the tube, which was heated in the absence of gas. Fluorescence excitation spectra were recorded using the fundamental (for detection of CCl_2) or frequency-doubled (for detection of CCl) output of a Nd: YAG (yttrium aluminum garnet) laser pumped dye laser (Continuum ND6000 or Lambda Physik LPD3002); the laser beam intersected the molecular source perpendicularly 1.5 cm downstream of the source. Fluorescence emitted perpendicular to both the molecular and laser beams was imaged into the entrance slit of a $\frac{1}{4}$ m monochromator and detected with a photomultiplier, whose output was directed to a gated integrator and then to a computer. As discussed previously,[14] the laser pulse energies employed were sufficiently low to avoid saturation effects.

Photolysis light at wavelengths near 248 nm was generated by either an excimer laser (Lambda Physik COMPex, operated with a KrF fill) or a tunable frequency-doubled Nd:YAG laser pumped dye laser (Continuum ND6000). The photolysis and probe laser beams were arranged to counterpropagate through the molecular beam apparatus perpendicular to the molecular beam direction. The delay between the photolysis and probe lasers was 70 ns. The available photolysis laser energy density was greater with the excimer laser (25 mJ in a 0.5 cm diameter beam) than with the frequency-doubled dye laser (1 mJ in a 0.3 cm diameter beam).

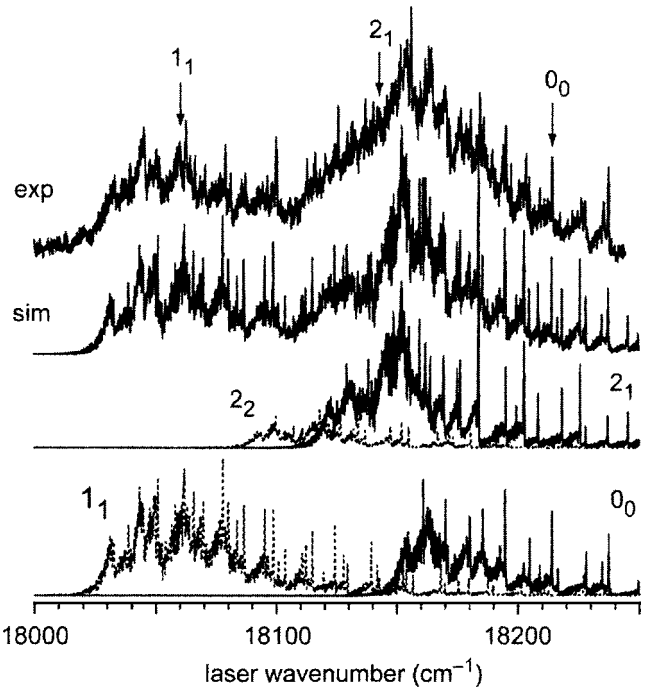

FIG. 1. Laser fluorescence excitation spectrum (upper trace) of the $\tilde{A}$-$\tilde{X}$ 2_0^3, $1_0^1 2_0^1$, 2_1^4, $1_0^1 2_1^2$, $1_1^0 2_0^5$, $1_1^1 2_0^3$, $1_1^2 2_0^1$, $1_1^2 2_0^1$, 2_2^5, and $1_0^1 2_2^3$ bands of the CCl_2 molecule, formed by pyrolysis of $CHCl_3$ (5% in argon) in a pulsed molecular beam source at 1 atm backing pressure. The sharp features in the spectrum are *Q*-branch subband heads of the $C^{35}Cl_2$ and $C^{35}Cl^{37}Cl$ isotopomers. The trace marked "sim" is a simulated spectrum which was constructed to reproduce the experimental spectrum. The simulated spectrum has contributions due to excitation from the $0_0, 2_1, 1_1, 2_2$ vibrational levels (shown as solid and dotted traces in the lower part of the figure). A rotational temperature of 40 K was employed in the simulations, and a Gaussian function with full width at half maximum (FWHM) 0.2 cm^{-1} was used to describe the laser frequency profile. The vertical arrows indicate the wavenumbers at which several vibrational levels were detected in the measurement of attenuation cross sections and their relative concentrations as a function of the temperature of the pyrolysis beam source (see text).

III. RESULTS

A. The CCl_2 parent molecule

The parent CCl_2 molecule was detected by laser fluorescence excitation in its $\tilde{A}\ ^1B_1$-$\tilde{X}\ ^1A_1$ band system[19–21] in order to probe the efficiency of production of CCl_2 in the beam source and to allow measurement of attenuation cross sections for various CCl_2 vibrational levels. In a previous study,[14] we recorded CCl_2 laser fluorescence excitation spectra in the 19 350–19 530 cm^{-1} wavenumber region. In this spectral range, hot bands were not observed, and we have shifted to a somewhat lower wavenumber range to find wavenumbers at which both the CCl_2 ground 0_0 and several excited vibrational levels could be selectively detected with good signal-to-noise ratio.

Figure 1 presents a laser fluorescence excitation spectrum in the 18 000–18 250 cm^{-1} wavenumber region. In this spectral region, the 0_0 vibrational level can be detected in the 2_0^3 and $1_0^1 2_0^1$ bands; the 2_1 level by the 2_1^4 and $1_0^1 2_1^2$ bands; the

1_1 level by the $1_1^0 2_0^5$, $1_1^1 2_0^3$, and $1_1^2 2_0^1$ bands; and (weakly) the 2_2 level by the 2_2^5 and $1_0^1 2_2^3$ bands. In order to determine the optimum transition wavenumbers for selective detection of the various vibrational levels, the recorded spectrum was compared to a simulated spectra, which were computed using the program ASYROTWIN.[22] The rotational constants of the ground vibronic level were taken from values obtained by microwave spectroscopy,[23] while the constants for vibrationally excited levels were obtained from values derived from analysis of $\tilde{A}$-$\tilde{X}$ spectra.[19,21] When available, rotational constants and band origin transition wavenumbers were taken from the high-resolution study by Clouthier and Karolczak.[19] Transition wavenumbers and excited-state *A* rotational constants for some bands were obtained from the work of Guss *et al.*[21] The simulations included bands from the $C^{35}Cl_2$ and $C^{35}Cl^{37}Cl$ isotopomers. Following our previous study[14] and consistent with the presently recorded spectra, a rotational temperature of 40 K was assumed in the simulations.

The relative intensities of the bands included in the simulations were varied until a reasonable representation of the experimental spectrum was achieved. The simulated spectrum and the contributions from excitation of the individual $CCl_2(\tilde{X}\,^1A_1)$ vibrational levels are displayed in Fig. 1, and compared to the experimental spectrum. From these simulations, appropriate wavenumbers were chosen for selective detection of specific vibrational levels. We note that the contribution to the spectrum from bands involving excitation of the 2_2 level is weak, and there is no wavenumber at which this level can be cleanly detected. It was not possible to determine the $CCl_2(\tilde{X}\,^1A_1)$ vibrational populations from the relative intensities of the bands since Franck–Condon factors for the relevant vibronic transitions are not available. Under similar beam conditions, the vibrational temperature of CFCl was found[16] to be 1050 ± 95 K.

In previous work,[15] we determined the 248 nm attenuation cross section for the CCl_2 0_0 level from the dependence of the CCl_2 laser fluorescence signal on the fluence of the photolysis (KrF excimer) laser. Here, we extend this measurement to the 2_1 and 1_1 levels, as well as report a new determination for the 0_0 level for comparison. Figure 2 presents a semilogarithmic plot of the measured dependence of laser fluorescence signals for detection of the CCl_2 0_0, 2_1, and 1_1 levels on the fluence of the 248 nm excimer laser. An iris was used to define the area *A* of the photolysis laser beam, and the pulse energy E_p was measured by placing a power meter inside the vented vacuum chamber. For each level, the attenuation cross section σ was determined by a weighed linear least squares fit of the logarithm of the CCl_2 signal versus laser fluence, following the relationship[24]

$$N_e = N_a \exp(-\sigma F), \tag{1}$$

where N_a and N_e are the concentrations of the $CCl_2(\tilde{X})$ vibrational level with the excimer laser off and on, respectively, and $F = E_p/(Ah\nu)$ is the laser fluence. The following values of σ were obtained: $(8.48 \pm 0.31) \times 10^{-18}$ cm^2 for the 0_0 level, $(2.01 \pm 0.19) \times 10^{-18}$ cm^2 for the 2_1 level, and $(2.47 \pm 0.19) \times 10^{-18}$ cm^2 for the 1_1 level. The determined

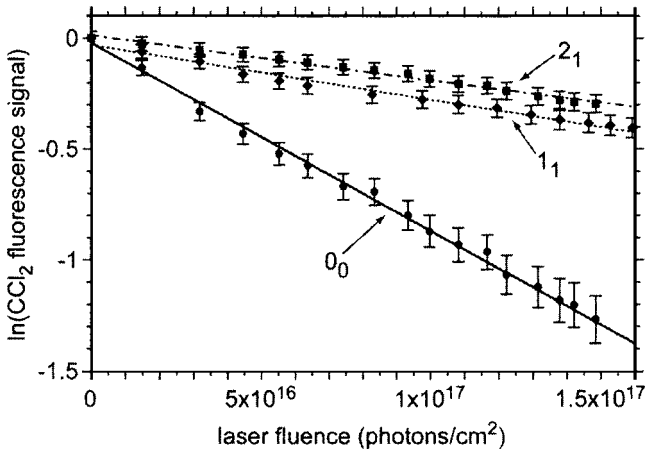

FIG. 2. Semilogarthmic plots of CCl_2 laser fluorescence signals as a function of the 248 nm excimer laser fluence: 0_0 level, circles; 2_1 level, squares; 1_1 level, diamonds. The wavenumbers at which these vibrational levels were detected are indicated in Fig. 1. The plotted lines are weighed linear least squares fits to determine attenuation cross sections.

cross sections for the excited vibrational levels are significantly smaller than for the 0_0 level. The present value for the 0_0 level is somewhat lower than previously reported[15] but within the experimental uncertainty. If the probability for excited-state dissociation is unity, then these cross sections can be equated with absorption cross sections. We see a strong variation of the cross sections for the different CCl_2 vibrational levels.

B. The CCl photofragment

A clear indication that the CCl photolysis fragments originate from two (or more) parent molecules comes from laser fluorescence excitation spectra recorded under identical conditions, except for the mole fraction of $CHCl_3$ in the gas mixture fed to the pyrolysis beam source. Figure 3 presents a series of CCl fluorescence excitation spectra taken under identical conditions, with the $CHCl_3$ mole fraction in the source gas mixture ranging from 5% down to 0.05%. It can be seen that the signals in the high-*J* portions of the P_1 and P_2 branches, which are marked in Fig. 3, have increasing intensity relative to the low-*J* portion of the F_1 subband as the $CHCl_3$ mole fraction is reduced. The varying ratios of the two classes of CCl fragments indicate that these arise from the photolysis of different parent molecules, whose concentrations vary with the $CHCl_3$ mole fraction in the beam source gas mixture.

The ratio of CCl low-*J* to high-*J* signals as a function of the $CHCl_3$ mole fraction in the source gas mixture is plotted in Fig. 4(a). It can be seen that this ratio extrapolates to a nonzero value for a source gas containing no $CHCl_3$. This suggests that the CCl high-*J* and a portion of the low-*J* fragments arise from the photolysis of a nascent product of the pyrolysis of $CHCl_3$, which we identify as CCl_2, as discussed previously[15] and in greater detail in Sec. III C. Under all experimental conditions investigated, the CCl laser fluorescence excitation spectra showed clear evidence for the two

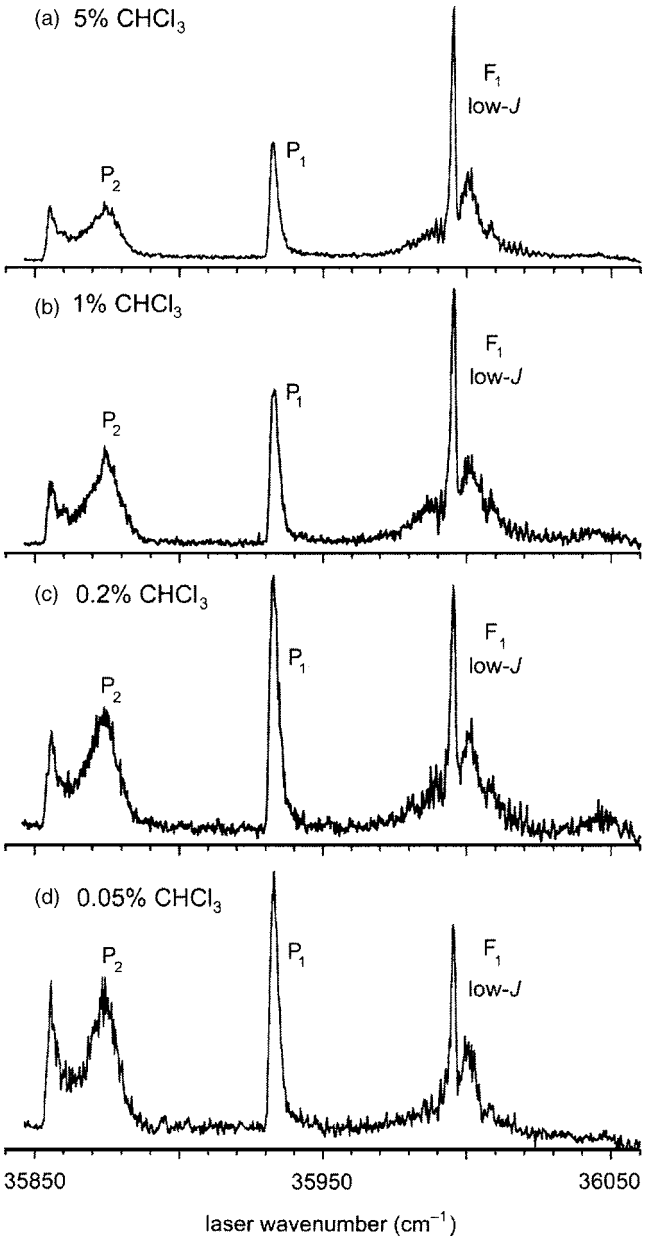

FIG. 3. Laser fluorescence excitation spectra of the CCl($X\ ^2\Pi$) product from the photolysis (248 nm excimer laser, fluence 4×10^{16} photons/cm^2) of a pyrolysis beam (estimated temperature of pyrolysis tube 1270 K) at a source backing pressure of 1 atm with $CHCl_3$ mole fraction (in argon) of (a) 5%, (b) 1%, (c) 0.2%, and (b) 0.05%. The wavelength regions of the high-J portions of several rotational branches, as well as the low-J portion of the F_1 subband, of the $A\ ^2\Delta$-$X\ ^2\Pi$ (0,0) band are indicated.

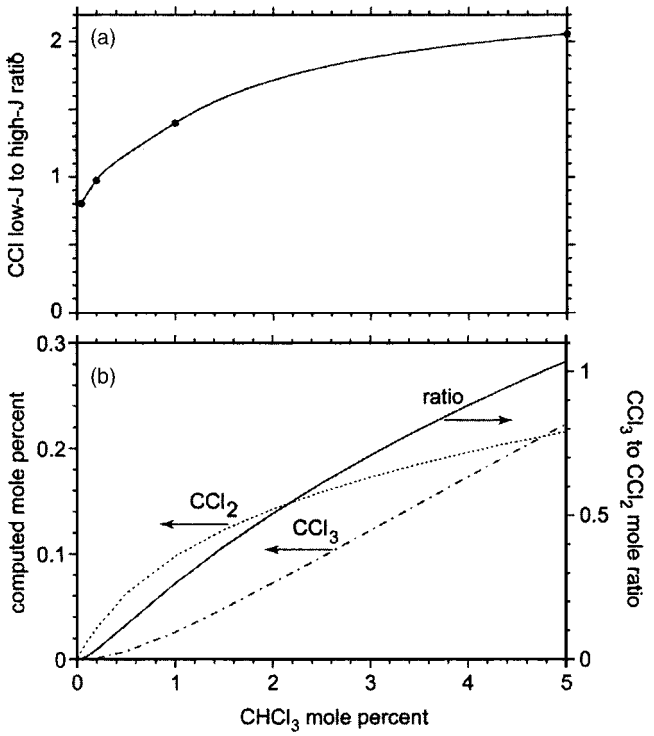

FIG. 4. (a) Ratio of the intensities of spectral features in Fig. 3 due to CCl low-J and high-J fragments (peak intensities of the low-J portion of the F_1 subband and P_1 branch) as a function of the $CHCl_3$ mole percent in the source gas mixture. A line has been interpolated through the plotted points to guide the eye. (b) Mole fractions of CCl_2 (dotted line) and CCl_3 (dot-dashed line) as a function of source gas $CHCl_3$ mole fraction, computed in kinetic simulations to model the pyrolysis of $CHCl_3$ in the source. The reaction mechanism of Kumaran *et al.* (Ref. 28), supplemented with reactions involving the $CHCl_2$ radical from Won and Bozzelli (Ref. 27) was employed in the simulations. The temperature and pressure were taken to be 1270 K and 1 atm, respectively, with a reaction time of 25 μs. The solid line displays the ratio of CCl_3 and CCl_2 mole fractions.

distinct groups of rotational levels in the CCl photofragment rotational state distribution, as observed and discussed in detail in our previous study.[15]

We have investigated the dependence of the CCl low-J and high-J laser fluorescence signals on the fluence of the photolysis excimer laser. Figure 5 presents these data for the two classes of CCl fragments. These data were recorded with a $CHCl_3$ mole fraction in the source gas of 0.05%, so that the photolytic precursor of the CCl low-J and high-J fragments was the nascent product of $CHCl_3$ pyrolysis. We see in Fig. 4(a) that the fluence dependence of the signal for the detection of high-J fragments is well described by a linear fit. At high laser fluences, we expect that the photofragment signal could deviate from a linear dependence on the fluence because of depletion of the parent molecules. Following Eq. (1), we expect the photofragment signal to have the following dependence on the photolysis laser fluence:

$$N_p = N_a[1 - \exp(-\sigma F)], \tag{2}$$

where N_p is the concentration of the photofragment. For low values of the product of the fluence F and the absorption cross section σ of the parent molecule, Eq. (2) reduces to a linear dependence of N_p on F, as observed in Fig. 4(a).

For the CCl high-J fragments, it is useful to apply Eq. (2) and inquire how large an absorption cross section would be consistent with the data plotted in Fig. 5(a), given the experimental uncertainties. The dotted line in Fig. 5(a) shows a calculated photofragment signal versus laser fluence using Eq. (2) with $\sigma=2.5\times10^{-18}$ cm^2. This suggests that the CCl high-J photofragments arise from photolysis of a parent molecule whose 248 nm absorption cross section is $\leqslant 2.5\times10^{-18}$ cm^2.

Figure 5(b) presents a plot of the dependence of the CCl low-J laser fluorescence signal on the fluence of the photolysis excimer laser. It can be seen that the data display a distinct curvature over the range of laser fluences investigated.

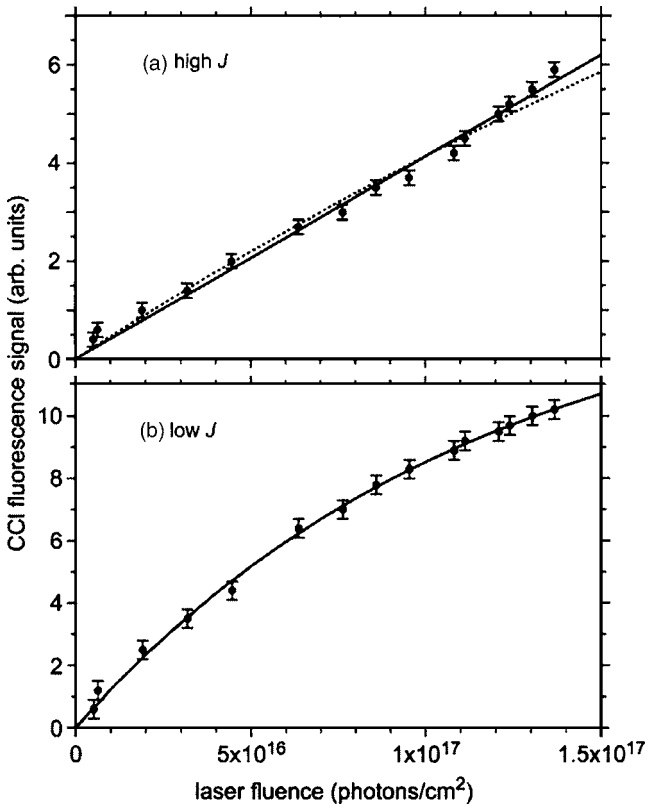

FIG. 5. Variation of CCl laser fluorescence intensity with the photolysis laser (248 nm excimer laser) fluence: (a) high-J fragments, detected in the P_1 branch of the A-X (0,0) band at 35 933 cm^{-1}, (b) low-J fragments, detected in the Q_1 branch of the A-X (0,0) band 35 996 cm^{-1}. In panel (a), the solid line is a linear fit, while the dotted line was computed using Eq. (2) with $\sigma=2.5\times10^{-18}$ cm^2. In panel (b), the solid line is a fit of the data to Eq. (2) with $\sigma=8.73\times10^{-18}$ cm^2. The source seed gas for both sets of data was 0.05% $CHCl_3$ in Ar at 1 atm total pressure, and the estimated temperature of the pyrolysis tube was 1270 K.

We fitted these data to Eq. (2) and found that a value $\sigma=(8.73\pm0.21)\times10^{-17}$ cm^2 yields a good representation of the data [solid line in Fig. 5(b)].

C. Identity of the precursors

Modern studies of the thermal dissociation of $CHCl_3$ have concluded that the initial step is molecular elimination to form CCl_2+HCl.[25–28] Kumaran *et al.*[28] and Won and Bozzelli[27] have constructed detailed reaction mechanisms to explain their observations. We have carried out kinetic simulations using the mechanism developed by Kumaran *et al.*[28] to describe the pyrolysis of $CHCl_3$ diluted in Kr. This mechanism should be similarly applicable to the pyrolysis of $CHCl_3$ in Ar. The mechanism was supplemented with reactions involving the $CHCl_2$ radical from Won and Bozzelli[27] in order to predict the concentrations of species produced in our pyrolysis beam source. The CHEMKIN suite of programs[29] was employed to solve the differential rate equations governing the time-dependent concentrations. The rate equations were integrated with initial conditions of 1270 K (typical operating temperature of the pyrolysis tube) and a pressure of 1 atm. The reaction time was taken to be 25 μs, which was estimated from the pyrolysis tube length and the sonic velocity. The principal pyrolysis products in the flow were computed to be the nascent CCl_2 product, as well as CCl_3, C_2Cl_2, and C_2Cl_4, which are formed through secondary reactions. The concentration of $CHCl_2$ was found to be negligible in the kinetic simulations under these conditions. The C_2 compounds cannot form CCl in a one-photon dissociation process at 248 nm, and hence, can be eliminated from consideration as photolytic precursors of CCl.

Figure 4(b) presents a plot of the mole fractions of CCl_2 and CCl_3 emanating from the pyrolysis tube as a function of the $CHCl_3$ mole fraction in the source gas mixture, as computed in our kinetic simulations. Also plotted in Fig. 4(b) is the computed CCl_3 to CCl_2 mole ratio. Since CCl_3 is a secondary decomposition product, it can be seen that this mole ratio is predicted to become very small as the $CHCl_3$ mole fraction is reduced, with a value of the ratio less than 0.01 for $CHCl_3$ mole fractions less than 0.1%.

It is interesting to compare the dependence of the computed CCl_3 to CCl_2 mole ratio and the observed ratio of CCl low-J to high-J signals on the $CHCl_3$ mole fraction in the source gas mixture, displayed in Figs. 4(b) and 4(a), respectively. Since the ratio of CCl low-J to high-J signals extrapolates to a nonzero value for a zero $CHCl_3$ mole fraction in the source gas, we conclude that CCl_2 is the photolytic precursor to CCl low-J fragments for low $CHCl_3$ mole fractions. At higher $CHCl_3$ mole fractions, photolysis of CCl_3 also contributes to the formation of low-J CCl fragments. We note also that our data support our previous conclusion[15] that the photolytic source of high-J CCl fragments is CCl_2.

Energetic considerations dictate the possible dissociation pathway for the formation of CCl in the 248 nm photolysis of CCl_3. The CCl fragment can be formed by the process

$$CCl_3 \rightarrow CCl + Cl_2, \quad \Delta H^\circ_{298} = 368 \text{ kJ mol}^{-1}. \qquad (2')$$

A similar molecular elimination process (formation of $CH+Br_2$) was observed[30] in the 193 nm photodissociation of $CHBr_2$, which itself was generated by photolysis of $CHBr_3$ in the same laser beam. It should be noted that there is not sufficient energy in the one-photon 248 nm photolysis of CCl_3 to allow formation of CCl+2 Cl fragments.

The room-temperature absorption spectrum of CCl_3 has been reported in two published studies.[31,32] The absorption cross section in the UV reaches a maximum value of $(1.45\pm1.5)\times10^{-17}$ cm^2 at 210 nm and has a value of $\sim2\times10^{-18}$ cm^2 at 248 nm. As discussed above, the molecular vibrational temperature in our beam is considerably above room temperature, likely slightly above 1000 K.[16] We expect, in general, that absorption cross section on the red side of an electronic transition increases with temperature.[33,34] However, it is unlikely that the cross section would grow as large as that at the maximum in a transition at the elevated vibrational temperatures of CCl_2 in our beam.

From our data, we deduce that both low-J and high-J CCl fragments are formed in the 248 nm photolysis of CCl_2, as we concluded in our initial study[15] of this process. However, the dependence of the low-J and high-J CCl signals on the photolysis laser fluence differ. This suggests that there are two separate precursors, possibly different vibrational levels of CCl_2, to these two classes of fragments. We note that the attenuation cross section determined for the ground

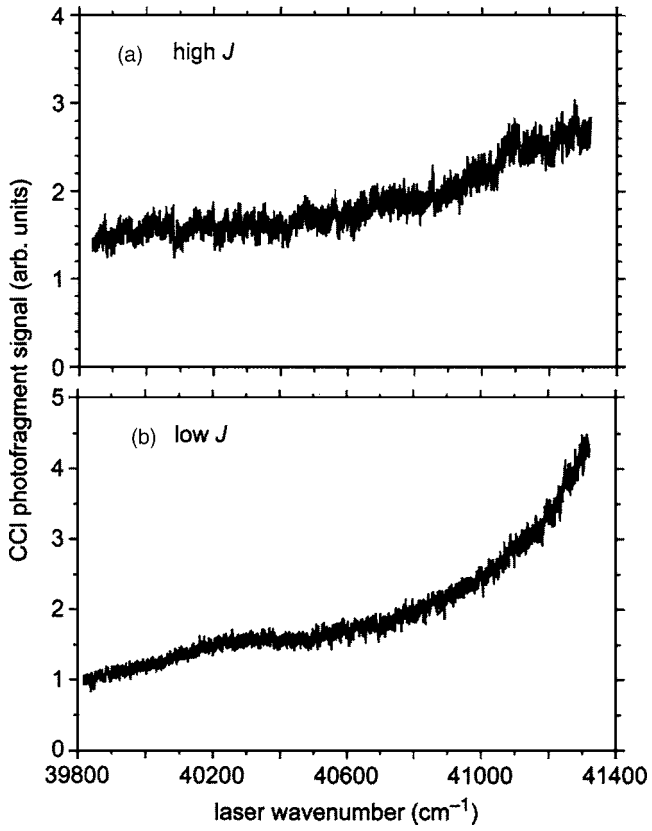

FIG. 6. Photofragment excitation spectra of (a) CCl high-J and (b) CCl low-J fragments, detected by laser fluorescence excitation in the P_1 branch (35 933 cm^{-1}) and the Q_1 branch (35 996 cm^{-1}) of the A-X (0,0) band, respectively. The spectra were recorded with an average photolysis laser fluence of 1.8×10^{16} photons/cm^2 and were corrected for the slight variation in photolysis laser energy with wavenumber.

vibronic 0_0 level of CCl_2 is much larger those for the 2_1 and 1_1 vibrationally excited levels [see Sec. III A]. In fact, the attenuation cross section obtained from the 0_0 level $[(8.48\pm0.31)\times10^{-18}$ cm$^2]$ is very close to the value fitted to the fluence dependence of the CCl low-J signals $[(8.73\pm0.21)\times10^{-17}$ cm$^2]$. This comparison strongly suggests that the 0_0 level of CCl_2 as the CCl low-J photolytic precursor.

From the essentially linear dependence of the CCl high-J laser fluorescence signals on the photolysis laser fluence, the precursor for these photofragments should have an absorption cross section $\leqslant2.5\times10^{-18}$ cm^2. On the basis of the measured attenuation cross sections for CCl_2 vibrational levels (see Sec. III A), likely candidates are vibrationally excited CCl_2 molecules. It is not possible to assign the CCl high-J photolytic precursor specifically to the CCl_2 2_1 and/or 1_1 levels since these both have absorption cross sections of the requisite magnitude.

D. Photofragment excitation spectrum

We have employed a tunable photolysis laser in order to probe the formation of CCl fragments as a function of wavelength around 248 nm. Figure 6 displays CCl photofragment excitation spectra for the detection of high-J and low-J fragments. These scans were taken with low photolysis laser fluence, so that the detected low-J fragments arose primarily from photolysis of the precursor with large absorption cross section, i.e., the CCl_2 0_0 ground vibronic level. We note that the central wavenumber of the excimer laser emission ($\sim$40 300 cm^{-1}) falls in the middle of the scanned spectral region.

The excitation spectra for both classes of CCl fragments are structureless, and the intensities increase with increasing photolysis laser wavenumber. We see in Fig. 6 that the intensity of the low-J fragment has a more rapid increase with wavenumber than for the high-J fragment. The lack of structure in the photofragment excitation spectra suggests that the excited electronic state dissociates directly, with a potential energy surface which is purely repulsive in the C–Cl coordinate.

IV. DISCUSSION

The present study amplifies and extends our previous study[15] of the photodissociation dynamics of CCl_2 near 248 nm. We have obtained direct evidence that there are several precursors to the observed CCl photofragments. We also observe that the 248 nm absorption cross sections for ground and vibrationally excited $CCl_2(\tilde{X})$ are dramatically different.

Some information is available on the relevant CCl_2 excited electronic states from *ab initio* calculations. Cai *et al.*[35] have computed adiabatic and vertical excitation energies for excited valence states. Eisfeld[36] has recently carried out a preliminary investigation of the dissociation pathways for excited singlet states. Above the well characterized ground $\tilde{X}\,^1A_1$ and first excited $\tilde{A}\,^1B_1$ singlet states[19–21] lie several excited singlet valence states. These include the $\tilde{B}\,^1A_2$ and $\tilde{C}\,^1B_2$ states, which have computed[35] vertical excitation energies of 35 600 and 41 100 cm^{-1}, respectively. Eisfeld[36] has also located an additional state, denoted as $\tilde{D}\,^1A_1$, which lies in the same energy range as the $\tilde{C}\,^1B_2$ state. Of these higher electronic states, both the $\tilde{C}\,^1B_2$ and $\tilde{D}\,^1A_1$ states can be accessed from the ground $\tilde{X}\,^1A_1$ state by an electric-dipole allowed transition in C_{2v} geometry. Eisfeld[36] computes that these higher excited states are either strictly repulsive in the C–Cl coordinate, or possess a small barrier to dissociation, due to avoided crossings with higher states. Moreover, the $\tilde{C}\,^1B_2$ and $\tilde{D}\,^1A_1$ states cross in C_{2v} geometry (and have an avoided crossing in C_s geometry) in the Franck–Condon region.[36] The $\tilde{C}\,^1B_2$ state prefers a slightly smaller bond angle than the ground $\tilde{X}\,^1A_1$ state, while the $\tilde{D}\,^1A_1$ state prefers a linear geometry as the Cl–CCl separation increases, releasing 15 000–20 000 cm^{-1} in becoming linear. This angular dependence can explain the formation of CCl fragments with a high degree of rotational excitation.

The significant variation of the 248 nm absorption cross sections of the $CCl_2(\tilde{X})$ vibrational levels deserves comment. The values for the vibrationally excited 1_1 and 2_1 levels are dramatically smaller than for the zero-point level. It should be noted that the vibrational energies of the excited levels are modest (computed[37] harmonic values of 733 and 337 cm^{-1}, respectively), and total energies are correspondingly only

slightly different. Also, the symmetries of the ground and investigated excited vibrational levels are all A_1.

The cross sections are proportional to the overlaps of the lower-state vibrational wave functions with the continuum wave functions in the excited electronic state, provided that the electronic transition dipole moment does not depend significantly upon nuclear geometry.[38] The lack of structure in the photofragment excitation spectra (Fig. 6) suggest that the dissociation is a direct process through repulsive excited state(s), rather than predissociation of quasibound vibronic levels. (As noted above, both the excited $\tilde{C}\,^1B_2$ and $\tilde{D}\,^1A_1$ states are electric-dipole accessible from the ground electronic state.) The differing values of the absorption cross sections could be the result of a large geometry change between the ground and excited electronic states, or a transition moment function which varies significantly with nuclear geometry. As an example of the latter, Levchencko *et al.*[39] found a strong enhancement in the absorption to the lowest $^2A_1$ state for vibrationally excited CH_2Cl. This was found to be due to a Rydberg-valence interaction in the excited state, which led to a strong geometry dependence of the transition moment function.

The equilibrium geometry computed by Cai *et al.*[35] for the $\tilde{C}\,^1B_2$ state is significantly different from that of the ground $\tilde{X}\,_1A_1$ electronic state, with a larger C–Cl bond length and a smaller bond angle [$\tilde{C}\,^1B_2$: $R(\mathrm{C-Cl})=2.02$ Å and $\theta(\mathrm{Cl-C-Cl})=94.7°$; $\tilde{X}\,_1A_1$: $R(\mathrm{C-Cl})=1.72$ Å and $\theta(\mathrm{Cl-C-Cl})=109.2°$]. This computed geometry change suggests that the overlap of the excited state and $\tilde{X}$ vibrational wave functions should be larger for the vibrationally excited levels than for the ground vibronic level. It is possible that the larger absorption cross section that we have determined for the ground vibronic level is due to mixing of excited electronic states, as in the case of CH_2Cl mentioned above. Such mixings are suggested in the preliminary calculations of Eisfeld.[36]

An even more dramatic difference between the 248 nm photodissociation of the ground and excited vibrational levels of CCl_2 is in the rotational state distribution of the CCl fragment. Our data strongly imply that CCl formed in the photodissociation of the excited vibrational levels is much hotter rotationally than is the case for the ground vibrational level. Unfortunately, we cannot experimentally identify the specific vibrational level(s), i.e., 2_1 and/or 1_1, which leads to the highly excited CCl fragments. However, taking the vibrational temperature previously deduced[16] for our CFCl beam, we estimate that the population of the 2_1 level in the beam is $\sim$1.7 times higher than that of the 1_1 level.

In view of the computed[36] avoided crossing of the $\tilde{C}\,^1B_2$ and $\tilde{D}\,^1A_1$ states in the Franck–Condon region, it is highly likely that nonadiabatic dynamics plays a significant role in the 248 nm photodissociation of CCl_2. Further details about the coupling of these and other excited electronic states should be forthcoming in the calculations being carried by Eisfeld.[36] Since the $\tilde{D}\,^1A_1$ state prefers a linear geometry at Cl–CCl separations greater than those of the avoided crossing, the high-J CCl fragments are likely formed by dissociation on this potential energy surface. The torques exerted on the dissociating molecule are less in the $\tilde{C}\,^1B_2$ state, and perhaps the low-J CCl fragments are by contrast generated by dissociation of this state.

The channeling of the flux of the dissociating molecule onto these two excited, dissociating electronic states is obviously dependent on the projection of the lower-state vibrational wave function onto the excited-state potential energy surface(s). In CCl_2, symmetry effects do not control the branching onto the two excited-state surfaces since the symmetries of the ground and excited vibrational levels are the same. Further insight into the detailed photodissociation dynamics of CCl_2 should become possible with the availability of further quantum chemistry calculations on the higher excited electronic states of this molecule.

For both low- and high-J CCl fragments, the action spectra show increasing intensities as a function of the photolysis laser wavenumber in the spectral region investigated (see Fig. 6). This indicates that the Franck–Condon maximum lies at a somewhat higher wavenumber.

We have also obtained information on the 248 nm photodissociation of the CCl_3 radical. It appears that this species dissociates to form CCl fragments that possess little rotational excitation. This is consistent with the $CCl+Cl_2$ dissociation channel [Eq. (2)], for which little torque is expected on the CCl fragment as the fragments dissociate. In our previous study,[15] we observed a significant effect of the backing pressure of the photolysis beam source upon the CCl state distribution, in particular, the F_1/F_2 fine-structure branching branching for the low-J component. This could result simply from a change in the rotational state distribution of the CCl_2 parent molecule with the beam conditions. Alternatively, the low-J CCl fine-structure branching could be different for photolysis of the CCl_2 0_0 level than that for the CCl_3 radical.

ACKNOWLEDGMENTS

This research has been supported in part by the National Science Foundation under Grant No. CHE-0413743. One of the authors (S.K.S.) gratefully acknowledges the Korea Science and Engineering Foundation for a postdoctoral fellowship. We are grateful to Professor Wolfgang Eisfeld for sharing the results of his preliminary calculations of CCl_2 dissociation pathways with us.

[1] See, for example, *Reactive Intermediate Chemistry*, edited by R. A. Moss, M. S. Platz and M. Jones, Jr. (Wiley-Interscience, Hoboken, NJ, 2004).
[2] H. Fan, C. Mukarakate, M. Deselnicu, C. Tao, and S. A. Reid, J. Chem. Phys. **123**, 014314 (2005).
[3] C. Tao, C. Mukarakate, and S. A. Reid, J. Chem. Phys. **124**, 224314 (2006).
[4] C.-S. Lin, Y.-E. Chen, and B.-C. Chang, J. Chem. Phys. **121**, 4164 (2004).
[5] Z. Wang, R. G. Bird, H.-G. Yu, and T. J. Sears, J. Chem. Phys. **124**, 074314 (2006).
[6] C. Tao, C. Mukarakate, and S. A. Reid, J. Mol. Spectrosc. **241**, 141 (2007).
[7] G. E. Hall, T. J. Sears, and H.-G. Yu, J. Mol. Spectrosc. **235**, 125 (2006).
[8] C. A. Richmond, J. S. Guss, K. Nauta, and S. H. Kable, J. Mol. Spectrosc. **220**, 137 (2003).
[9] C. Tao, C. Mukarakate, D. Brusse, Y. Mishchenko, and S. A. Reid, J. Mol. Spectrosc. **241**, 180 (2007).

[10] C. Tao, S. A. Reid, T. W. Schmidt, and S. H. Kable, J. Chem. Phys. **126**, 051105 (2007).
[11] J. S. Guss, O. Votava, and S. H. Kable, J. Chem. Phys. **115**, 11118 (2001).
[12] P. T. Knepp, C. K. Scalley, G. B. Bacskay, and S. H. Kable, J. Chem. Phys. **109**, 2220 (1998).
[13] P. T. Knepp and S. H. Kable, J. Chem. Phys. **110**, 11789 (1999).
[14] S. K. Shin and P. J. Dagdigian, J. Chem. Phys. **125**, 133317 (2006).
[15] S. K. Shin and P. J. Dagdigian, Phys. Chem. Chem. Phys. **8**, 3446 (2006).
[16] S. K. Shin and P. J. Dagdigian, J. Chem. Phys. **126**, 134302 (2007).
[17] S. K. Shin and P. J. Dagdigian, J. Chem. Phys. **128**, 064309 (2008).
[18] D. W. Kohn, E. S. J. Robles, C. F. Logan, and P. Chen, J. Phys. Chem. **97**, 4936 (1993).
[19] D. J. Clouthier and J. Karolczak, J. Chem. Phys. **94**, 1 (1991).
[20] M.-L. Liu, C.-L. Lee, A. Bezant, G. Tarczay, R. J. Clark, T. A. Miller, and B.-C. Chang, Phys. Chem. Chem. Phys. **5**, 1352 (2003).
[21] J. S. Guss, C. A. Richmond, K. Nauta, and S. H. Kable, Phys. Chem. Chem. Phys. **7**, 100 (2005).
[22] R. H. Judge and D. J. Clouthier, Comput. Phys. Commun. **135**, 293 (2001).
[23] M. Fujitake and E. Hirota, J. Chem. Phys. **91**, 3426 (1989).
[24] R. Rohrer and F. Stuhl, J. Chem. Phys. **88**, 4788 (1988).
[25] K. P. Schug, H. G. Wagner, and F. Zabel, Ber. Bunsenges. Phys. Chem. **83**, 167 (1979).
[26] I. P. Herman, F. Magnotta, R. J. Buss, and Y. T. Lee, J. Chem. Phys. **79**, 1789 (1983).
[27] Y. S. Won and J. W. Bozzelli, Combust. Sci. Technol. **85**, 345 (1992).
[28] S. S. Kumaran, M.-C. Su, K.-P. Lim, J. V. Michael, S. J. Klippenstein, J. DiFelice, P. S. Mudipalli, J. H. Kiefer, D. A. Dixon, and K. A. Peterson, J. Phys. Chem. A **101**, 8653 (1997).
[29] CHEMKIN, Release 4.1, Reaction Design, Inc., San Diego, CA ⟨www.reactiondesign.com⟩.
[30] P. Zou, J. Shu, T. J. Sears, G. E. Hall, and S. W. North, J. Phys. Chem. A **108**, 1482 (2004).
[31] F. Danis, F. Caralp, B. Veyret, H. Loirat, and R. Lesclaux, Int. J. Chem. Kinet. **21**, 715 (1989).
[32] T. Ellermann, Chem. Phys. Lett. **189**, 175 (1992).
[33] L. Brouwer, H. Hippler, L. Lindemann, and J. Troe, J. Phys. Chem. **89**, 4608 (1985).
[34] H. Hippler, D. Nahr, H. J. Plach, and J. Troe, J. Phys. Chem. **92**, 5503 (1988).
[35] Z.-L. Cai, X.-G. Zhang, and X.-Y. Wang, Chem. Phys. Lett. **210**, 481 (1993).
[36] W. Eisfeld, personal communication (6 October 2006).
[37] G. Tarczay, T. A. Miller, G. Czakó, and A. Császár, Phys. Chem. Chem. Phys. **7**, 2881 (2005).
[38] R. Schinke, *Photodissociation Dynamics* (Cambridge University, Press, Cambridge, 1993).
[39] S. V. Levchenko, A. V. Demyanenko, V. L. Dribinski, A. B. Potter, H. Reisler, and A. I. Krylov, J. Chem. Phys. **118**, 9233 (2003).